www.czasopisma.pan.pl PAN POLSKA AKADEMIA NAUK www.journals.pan.pl

Arch. Metall. Mater. **64** (2019), 3, 1117-1124

DOI: 10.24425/amm.2019.129503

R. KOŇÁR*#, M. MIČIAN*, M. BOHÁČIK*, M. GUCWA**

IDENTIFICATION OF LACK OF FUSION AND INCOMPLETE PENETRATION IN BUTT WELD JOINT BY ULTRASONIC PHASED ARRAY METHOD AND X-RAY METHOD

The main goal of the article is to identify artificially created defects like lack of fusion and incomplete penetration in butt weld joint using non-destructive volumetric methods. These defects are the most serious defects in welds of steel constructions from the safety point of view. For identification, an ultrasonic phased array technique and a conventional X-ray using digital imaging were used. The theoretical part of the article describes the current state of the given issue and provides basic theoretical knowledge about ultrasonic and X-ray welding tests. In the experimental part, the procedure and results of testing butt weld joint are described by both non-destructive methods. The butt weld joint was made from steel S420MC. Each indication obtained by the ultrasonic and x-ray technique is supplemented by the macrostructure of the weld taken from the indication position. The results of the experimental work mentioned in the article point to the possibility and reliability of the identification of melting defects by selected nondestructive methods in terms of their character and orientation.

Keywords: internal defects, butt weld joint, nondestructive testing, lack of fusion, incomplete penetration.

1. Introduction

In the manufacture of steel constructions and components by arc welding technology, welding defects are an integral part of manufacturing technology. There are many factors to the process of making a weld. By optimizing these factors, it is possible to minimize the presence of defects but cannot be completely eliminated. There has been an increasing trend in requirements for welded structures, a reduction in safety factors and the weight of structures by using higher strength steels in recent years. The use of higher strength steels increases the risk of failure of welded joints in the presence of defects, which can lead to dangerous and costly failures. Surface and volumetric non-destructive testing techniques should have to detect these defects during production and operation. We use a combination of surface methods, including visual, penetration and magnetic particle testing methods to identify surface and subsurface defects. Volumetric test methods include X-ray (RT) and ultrasonic testing (UT). UT testing has still greater representation in checking the quality of welded joints as X-ray testing. It is caused to the rapid development of UT techniques, especially modern digital UT defectoscopes, with the ability to create a record from the test results, automation of testing, new types of UT probes and innovative techniques of UT testing (TOFD – Time of Flight Diffraction and PA – Phased Array). Compared to RT, it allows performing relatively quick and inexpensive testing of weld joints without interrupting the production process. The advantage of UT testing is also the higher sensitivity to surface defects like lack of fusion an incomplete penetration compared to X-ray control. Current UT testing using PA technology provides much more options than standard UT testing, what is set up by specially designed probes with more transducers [1,2].

2. Phased array technique

Conventional UT transducers for non-destructive (NDT) commonly consist of either a single active element that both generates and receives high-frequency sound waves or two paired elements, one for transmitting and one for receiving. PA transducer is simply one that contains several separate elements in a single housing, and phasing refers to how those elements are sequentially pulsed. PA system is normally based around a specialized UT transducer that contains many individual elements (typically from 16 to 256) that can be pulsed separately in a programmed pattern. This probe construction design allows control the direction of the beam and also creates sectorial or linear scans [1,3,5].

These transducers may be used with various types of wedges, in a contact mode, or in immersion testing. Their shape may be square, rectangular, or round, and test frequencies are most commonly in the range from 1 to 10 MHz. Fig. 1 shows the difference between conventional and PA generated UT beam [1,5,6,8].

* UNIVERSITY OF ŽILINA, FACULTY OF MECHANICAL ENGINEERING, DEPARTMENT OF TECHNOLOGICAL ENGINEERING, UNIVERZITNÁ 1, 010 26 ŽILINA, SLOVAKIA
** CZESTOCHOWA UNIVERSITY OF TECHNOLOGY, INSTITUTE OF MECHANICAL TECHNOLOGIES, DĄBROWSKIEGO 69, 42-201 CZĘSTOCHOWA, POLAND
# Corresponding author: radoslav.konar@fstroj.uniza.sk

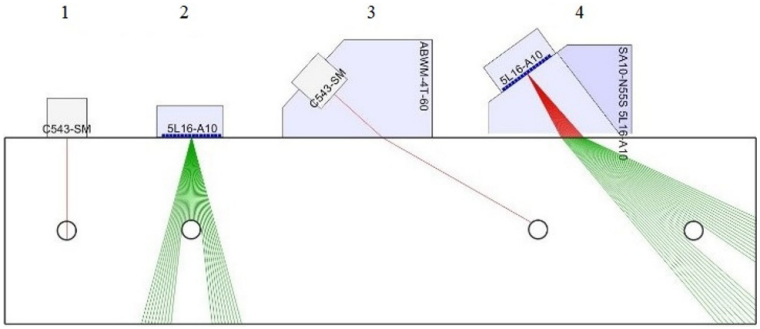

Fig. 1. The difference between conventional and phased array generated ultrasonic beam (1,3 – conventional ultrasound probes generated single beam scan, 2,4 – phased array probes generated sectorial scan)

3. X-Ray technique

X-Ray testing is one of the basic NDT methods to display real dimensions and the shape of errors found in the material. To check are using the physical properties of ionizing electromagnetic radiation (X-radiation, gamma radiation) with the matter of product and in subsequent visibility given ionizing radiation per controlled product through appropriate detector (classic radiographic film, flexible IP plate, flat digital detectors). The basic principle of radiography is illustrated in Fig 2.

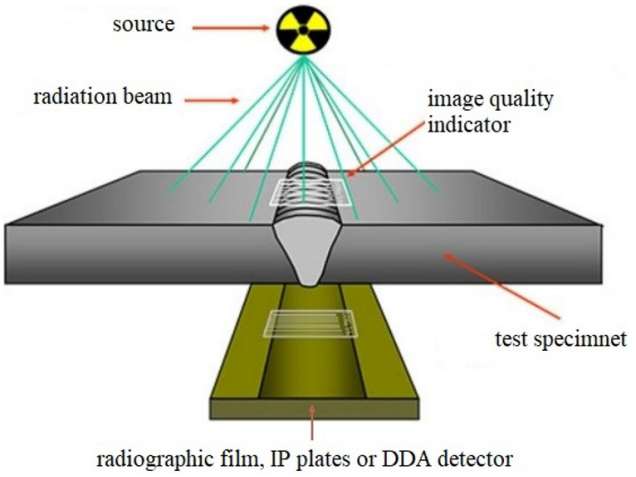

Fig. 2. The principle of radiography

Industrial radiology uses for NDT testing of materials mostly X-rays and gamma radiation. As a source of X-rays, they are most commonly used X-Ray tubes. The basic of roentgen is the X-ray lamp itself. The digitization of classic X-ray films is nowadays used to optimize and enhance the image quality of a classic X-ray image. Digitizing the X-ray image is performed using a scanner that allows transferring image data from the RTG film to a digital data format [4,5,9-11].

4. Experimental sample

The aim of the experimental work was to make a butt weld joint with artificially created defects that most often occur during welding and then to test them by selected volumetric non-destructive methods. The main parameter of artificially produced defects in butt weld joint was in order to coincide with the natural manufacturing defects as much as possible. Experimental sample from higher strength steel S420MC (Wr.N. 1.0980) was made for the volumetric defects identification such as lack of fusion and incomplete penetration [5,11,12].

The chemical composition and mechanical properties of the S420MC steel are in Tab. 1.

Sample dimensions were 300×250×10 mm. The welding surfaces have been prepared so that a butt weld joint can be formed between the steel sheets. The experimental sample was welded by butt weld with method 135 according to STN EN ISO 4063 (Metal active gas welding). Shielding gas with composition 82% Ar + 18% CO2 was used in welding. Filler material was wire G3Si according to STN EN ISO 14341-A with a diameter of 1 mm. The weld was made by 3 layers (5 weld beads). Weld joint preparation, weld macrostructure, sample dimensions, and sample testing sides are shown in Fig. 3.

During welding, defects such as lack of fusion and incomplete penetration defects were deliberately made in the sample. The sample was subjected to NDT testing after the welding. The

TABLE 1

Chemical composition and mechanical properties of S420MC steel

Chemical composition									
Element	**C**	**Si**	**Mn**	**P**	**S**	**Al**	**Nb**[1)]	**V**[1)]	**Ti**[1)]
[wt. %]	max. 0.120	max. 0.500	max. 1.600	max. 0.025	max.0.015	min. 0.015	max. 0.09	max. 0.20	max. 0.15
Mechanical properties									
Material and thickness			**State**		**R_m [MPa]**		**R_{eH} [MPa]**		**A [%]**
S420MC t ≥ 3			Thermo-mechanically rolled		480-620		420		19

[1)] Nb + V + Ti ≤ 0,22 %

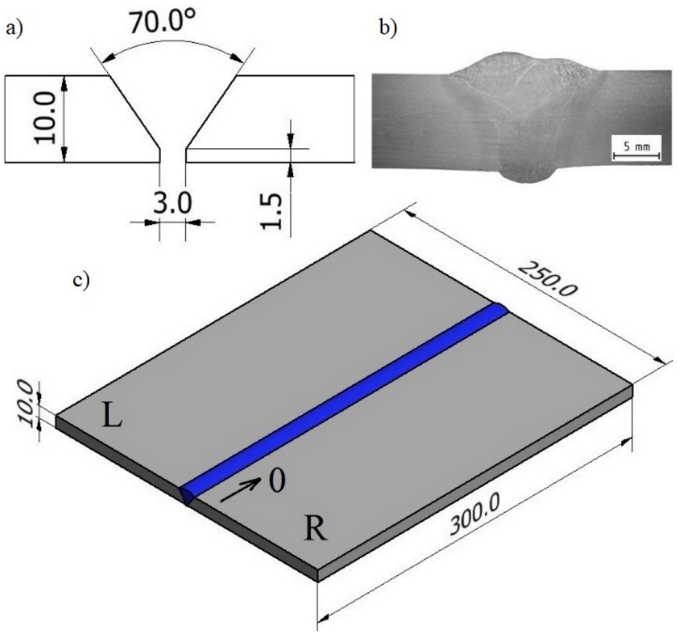

Fig. 3. Experimental sample: a) weld joint preparation, b) weld macrostructure, c) sample dimensions

permissibility of defects in welding according to EN ISO 5817 has not been evaluated. The main aim is to compare the display of the error on the UT and X-Ray record [3,5,7].

4.1. Sample testing by ultrasonic Phased array technique

Ultrasonic PA testing of the sample was performed at the Olympus MX2 16/64 (16 – the number of active management probe elements, 64 max. number of connected elements). 16 elements UT probe 5L16A10 with a frequency of 5MHz with the wedge SA 10-N55S (S – transverse waves, N55 – medium angle sector, SA 10 – wedge type specifically for that type of probe) was used for UT testing. Generated UT signal for middle probe element (8 elements) and Fourier signal transform is shown in Fig. 4. Generated UT signal has an average center frequency of 5.15 MHz and average –6dB bandwidth 81%.

Measured S-scan was set to the range of angles 40°-70°. EchoMix UT gel was used as coupler medium. Linear PA weld testing record was made using the encoder ENC1-2.5 with 12 steps on 1 mm. Basic amplification 23.6 dB have been set for UT testing. For the sensitivity of measurements was used curve DAC with side cylinder bore Ø3 mm. The position of the probe was simulated before testing in the program EC Beam Tool 5. Probe testing position must ensure testing the entire volume of the weld. The test was performed on both sides of the weld (L-left side, R-right side). Evaluation of the results was carried out in the software OmniPc 4.2 [5].

Places with representative defects were selected from the entire UT scan record. These defects were assigned to the appropriate S-scan and A-scan at the angle of the UT beam pointing to the maximum signal from the error. PA scan record is in Fig. 5.

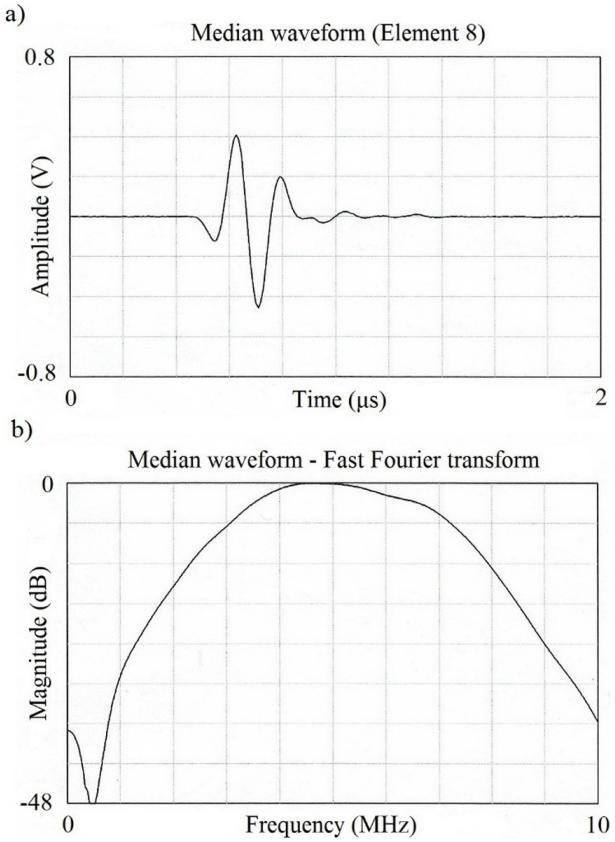

Fig. 4. Generated ultrasonic signal: a) signal shape, b) signal Fourier transform

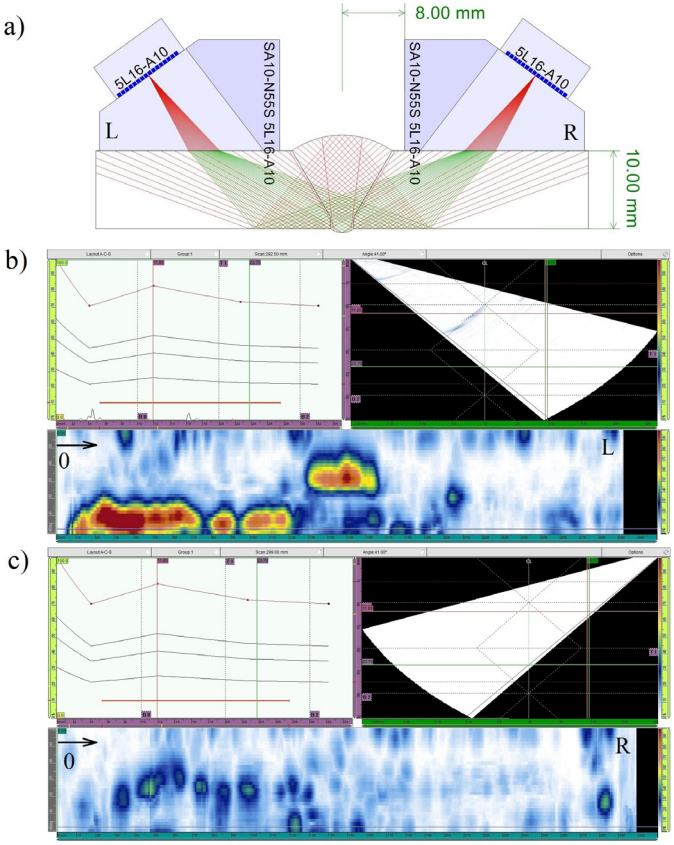

Fig. 5. PA scan record of the entire length of the weld: a) ultrasonic testing simulation and test probe position, b) left side probe position testing record, c) right side probe position testing record

4.2. Sample testing by X-Ray technique

X-Ray testing of the sample was performed after ultrasonic control. An Eresco X-ray lamp with 160kV / 5mA was used to perform the scanning. The sample's distance from the focus of the lamp was 700 mm and the exposure time was 5 min. Weld was testing once on 350×100 mm conventional radiographic film. X-Ray analog record (RTG film) was converted to a digital image by an X-ray film scanner. The software filter was used to highlight radiogram results. X-ray all weld record is in Fig. 6.

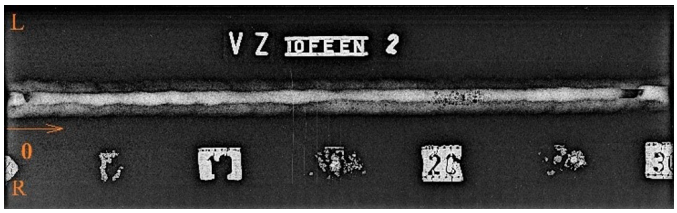

Fig. 6. X-ray testing record

5. Evaluate of the results

The result of the experimental part of this article are macrostructures of welds with artificially created defects with associated UT and X-ray indications. UT beam simulation is also assigned to each indication in the ES Beam Tool 5 program. The standard defect number according to EN ISO 6520-1 was assigned to each defect on macrostructure.

The reference macrostructure was removed at the flawless welding position in first. The reference macrostructure is shown in Fig. 7.

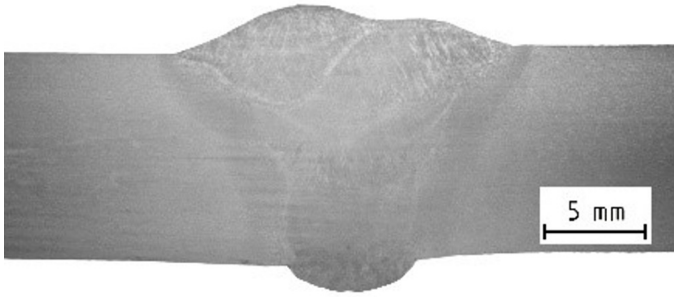

Fig. 7. Reference sample weld macrostructure

In the macrostructure, there are not defects classified in EN ISO 6520-1. UT recording from a flawless location is shown in Fig. 8.

On the PA record obtained from flawless macrostructure are not presented welding defects indications. The shape echo from the root or the surface of the welding joint may be visible on the record in some cases.

The reference sample of RTG record is shown in Fig. 9.

Even the X-ray record does not show the presence of the welding defect.

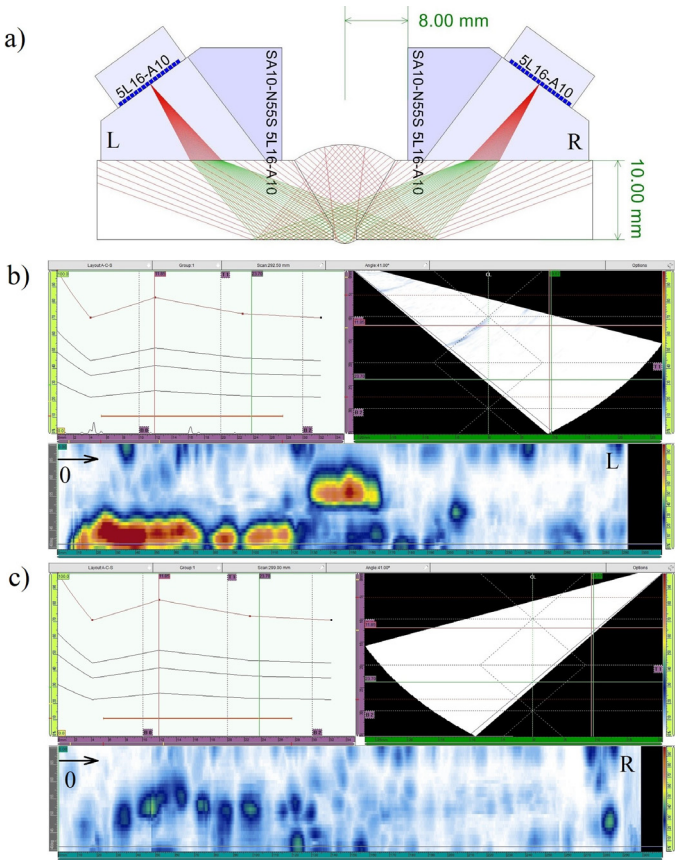

Fig. 8. Phased array S-scan from the reference sample: a) ultrasonic testing simulation and test probe position, b) left side probe position testing record, c) right side probe position testing record

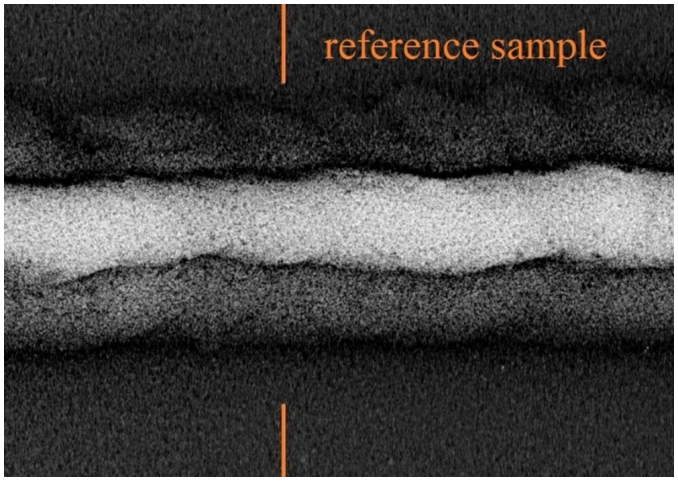

Fig. 9. X-ray reference sample record

The first evaluated defect in weld was lack of fusion (sample No.1). The sample No. 1 macrostructure is shown in Fig. 10. There are two defects No. 401 according to EN ISO 6520-1. These are internal surface defects with different orientation and minimal thickness.

The results of PA testing from both sides of the weld, as well as simulation of UT propagation in the sample with the defect, are shown in Fig. 11. The position of the butt weld on PA record is highlighted with orange color.

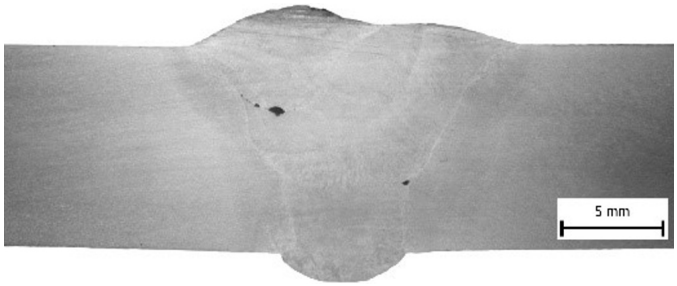

Fig. 10. Weld macrostructure of sample No. 1

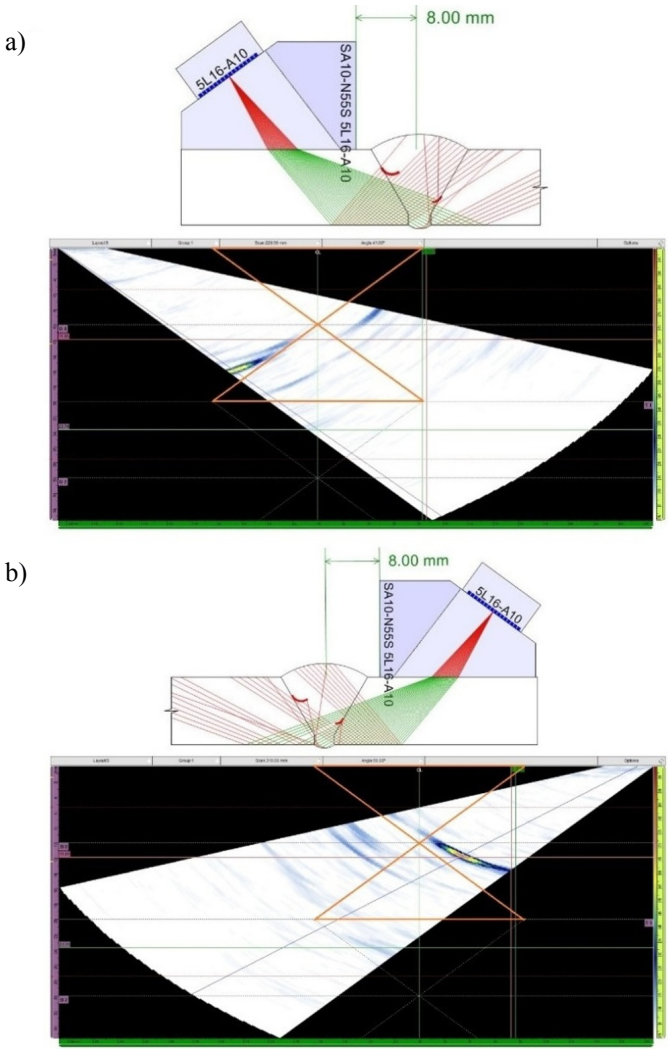

Fig. 11. Phased array S-scan from sample No. 1: a) left side probe position testing record, b) right side probe position testing record

X-ray sample No. 1 record is shown in Fig. 12.

Defects have been caused by insufficient melting of the welding area during welding. The main cause was the low welding speed, which caused the accumulation of molten metal in front of the electric arc. The defect indication of lack of fusion is clearly visible on the PA record, while the defect indication is not visible on X-ray record at all. Both defects are clearly visible at PA records. They will appear on the record by a color scale. The color scale is replaced by the height of the acoustic ultrasonic energy reflected by the defect.

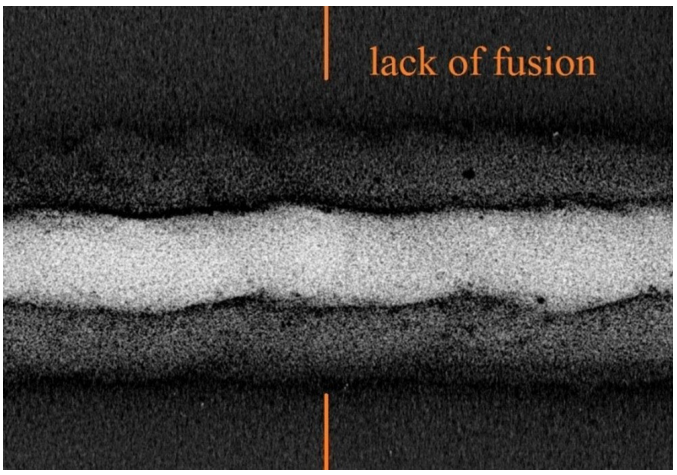

Fig. 12. X-ray sample No. 1 record

The position with a significant indication is indicated by a red color, the position without the indication is shown on PA record by a white color. The indication positions are identical to the defect position on macrostructure sample No. 1.

The defect is not displayed on X-ray record due to very low defect thickness – there was no radiation increasing for experimental sample. On an X-ray image can be seen only volumetric defects (cavity) above the lack of fusion defect.

The second evaluated defect was again lack of fusion in another location of the weld. The macrostructure No. 2 is shown in Fig. 13. There are three errors No. 401 marked according to EN ISO 6520-1 in the macrostructure of sample No. 2 These are internal surface defects with a different orientation.

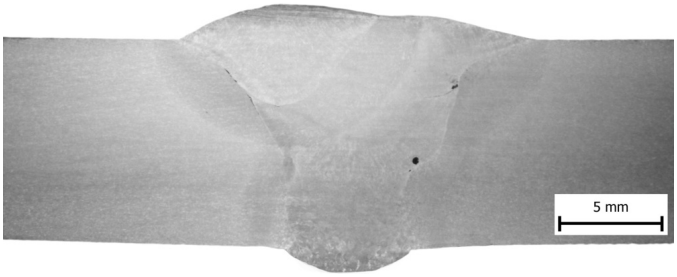

Fig. 13. Weld macrostructure of sample No. 2

It is possible to identify the defects present in the macrostructure as classified in EN ISO 6520-1. The results of UT testing from both sides of the weld, as well as simulation of UT propagation in the sample with the defect, are shown in Fig. 14.

X-ray record of sample No. 2 is shown in Fig. 15.

Even in this case, defects may have been caused by insufficient melting of the welding area during welding, by incorrect burner control and improper handling with it or could have been caused by a low welding speed. An indication of melting defects was more noticeable on the PA record.

The defects are clearly visible at PA records. They will appear on the record by a color scale. In this case, the melting defect is also displayed with a higher intensity of acoustic energy because it is a significant directional reflector. Volumetric

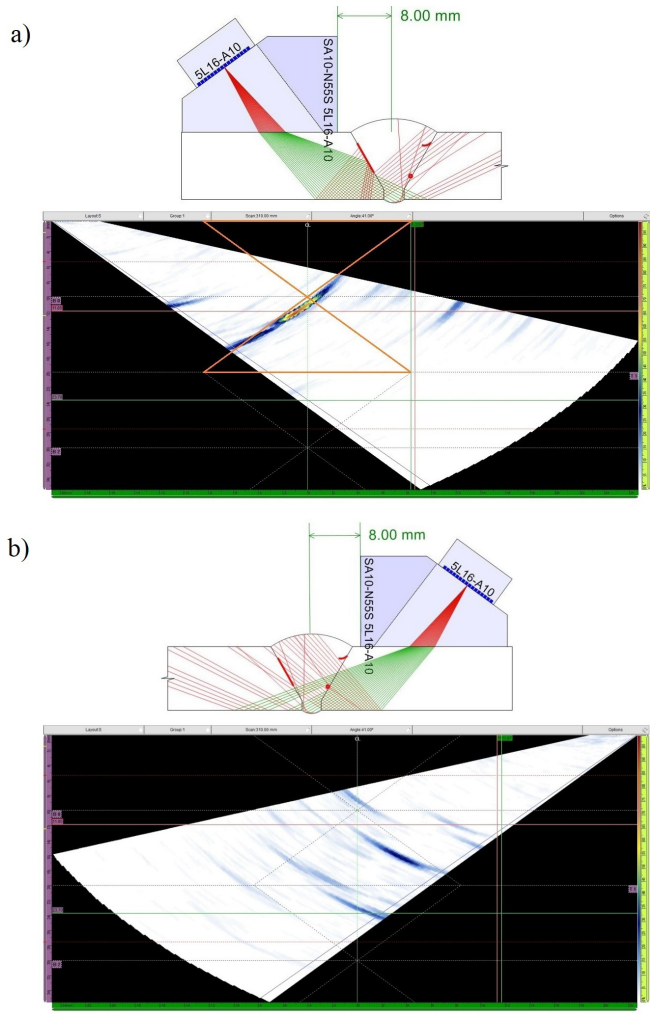

Fig. 14. Phased array S-scan from sample No. 2: a) left side probe position testing record, b) right side probe position testing record

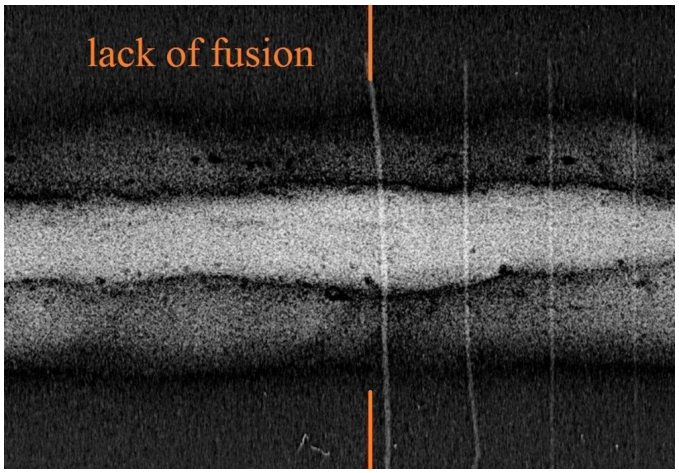

Fig. 15. X-ray sample No. 2 record

errors are not a significant directional reflector, therefore they will not appear so significantly as the defects that are significant directional reflectors. The position of the indications is identical to the defect position on macrostructure of sample No. 2.

Identify a surface defect on the X-ray record is not possible to because its minimum thickness did not show up like darker places of the film. On X-ray image can be seen only volumetric defects (pores) above the lack of fusion defect.

The third defect to evaluate was melting defect and clustered pores. The macrostructure of weld No. 3 is shown in Fig. 16. In the macrostructure of sample No. 3 there was defect No. 401 and defect No. 2013 marked according to EN ISO 6520-1. These are internal surface and volumetric defects with a different orientation.

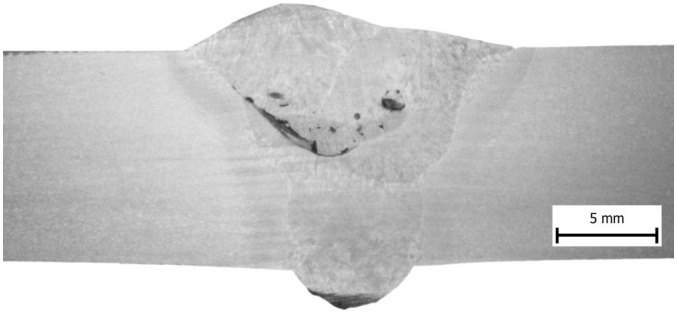

Fig. 16. Weld macrostructure of sample No. 3

The results of UT testing from both sides of the weld, as well as simulation of UT propagation in the sample No. 3 with the defect are shown in Fig. 17.

X-ray sample No. 3 record is shown in Fig. 18.

Pores are formed in MAG welding technology, especially in the insufficient gas protection of molten metal.

The melting defect is also displayed with higher intensity compared to pores because it is a significant directional reflector also in this case. From the point of view of pore identification and evaluation, this indication may be confused with the noise from the weld structure. The low intensity of echoes causes a spherical shape of pores that are not a significant directional reflector. For this reason, only a small part of the incident energy is reflected back into the probe. In the case of a change in the direction of the testing, the size of the reflected energy from the pores does not change. The position of the indications is identical to the position of the defect on macrostructure sample No. 3.

The clustered pores on the X-ray record are possible to identify because they are shown up like darker places on the film. Only volumetric defects can be seen in the X-ray image.

The fourth evaluated defect was lack of fusion and two-sided incomplete penetration in weld root. The macrostructure of weld sample No. 4 is shown in Fig. 19. There was defect no. 401 and defect no. 4021 marked according to EN ISO 6520-1 in the macrostructure of sample No. 4. These are internal surface defects with a different orientation.

Lack of fusion and incomplete penetration are possible to identify in the macrostructure. In the case of incomplete root penetration, it is a blunting of weld root which has not been melted. The defect could also be identified by visual inspection from the root of the welding joint.

The results of PA testing from both sides of the weld, as well as simulation of UT propagation in the sample with the defect, are shown in Fig. 20.

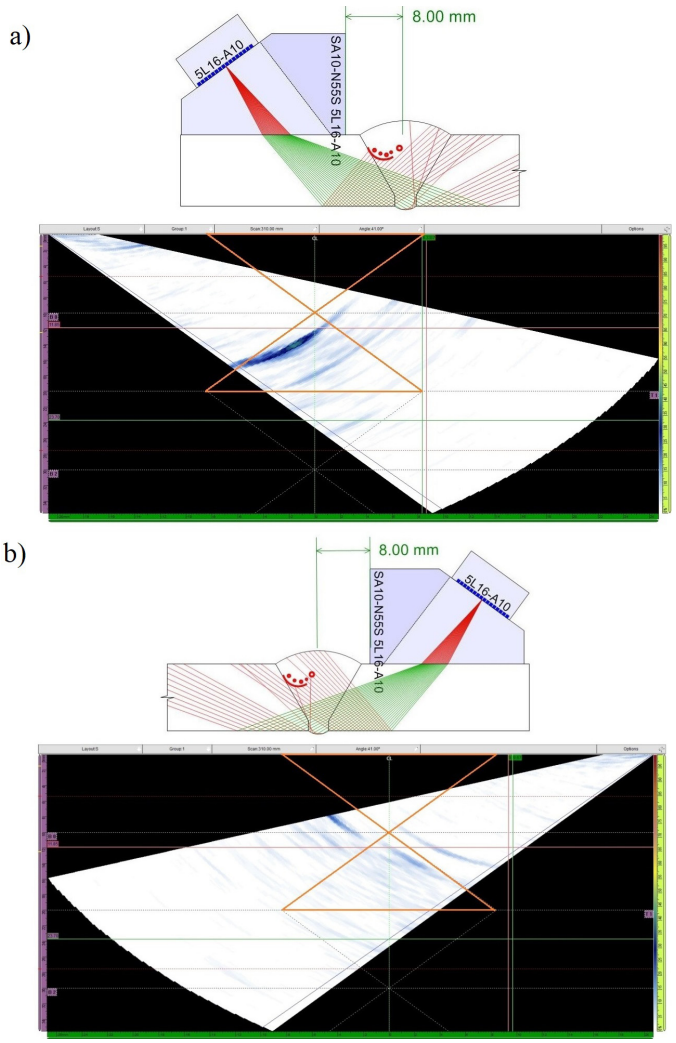

Fig. 17. Phased array S-scan from sample No. 3: a) left side probe position testing record, b) right side probe position testing record

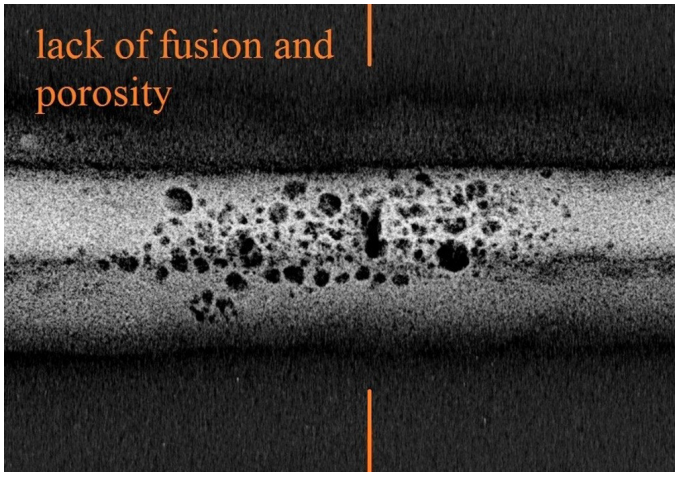

Fig. 18. X-ray sample No. 3 record

Sample No. 4 of X-ray record is shown in Fig. 21.

The defect was caused by incorrect welding of the root when welding the root layer. It was also identified by X-ray and PA control.

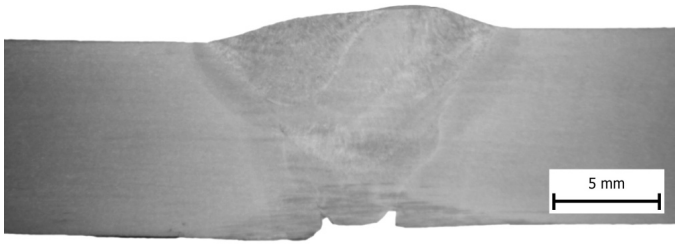

Fig. 19. Weld macrostructure of sample No. 4

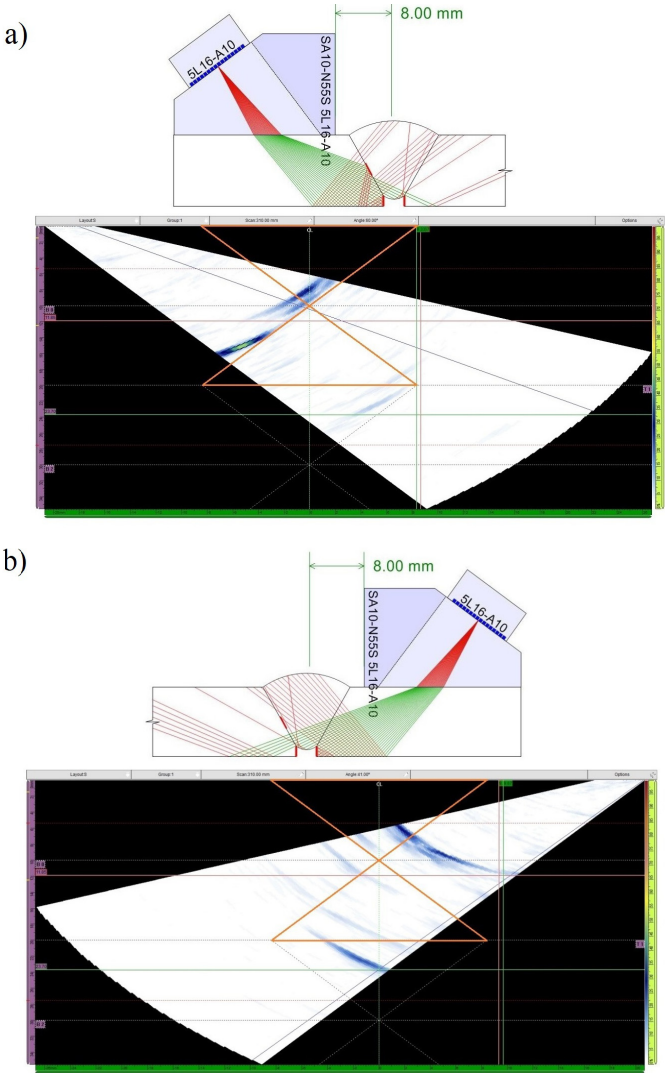

Fig. 20. Phased array S-scan from sample No. 4: a) left side probe position testing record, b) right side probe position testing record

Defects are clearly visible at PA records. They will appear on the record by a color scale. In this case, the surface defect is also displayed with higher intensity because it is a significant directional reflector. A more pronounced indication is on the left PA record, which is the result of the geometric shape of the incomplete penetration. The position of the indications is identical to the defect position on macrostructure of sample No. 4.

There is a two-sided incomplete penetration in weld root that is visible and can be uniquely identified on the X-ray scan record.

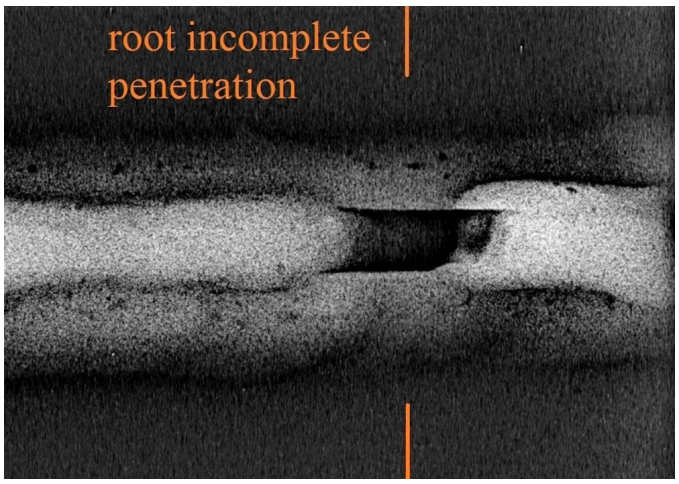

Fig. 21. X-ray sample No. 4 record

6. Conclusions

The aim of the article was to assign the corresponding indication obtained by the ultrasonic PA technique and the X-ray technique to the macrostructure with the defect. The recording obtained by PA technique is also supportive of simulation of ultrasound propagation in the PA program.

The main goal was also to compare the reliability of the PA and X-ray techniques from the point of view of surface and volume defects identification. It is clear from the results that surface defects on the X-ray record cannot be uniquely identified. Surface defects are uniquely identified by the PA technique with the correct setting of the measurement system.

Volume defects can be uniquely identified on X-ray record. Defects on PA record are hardly identifiable and can be exchanged with the noise from the structure. However, from the safety point of view, volume defects are less dangerous than surface defects.

The results of the experimental part of this article serve not only as a tool for NDT staff but also as an instruction for the correct choice of technique and methodology for butt welded joints testing.

REFERENCES

[1] R. Kaczmarek, R. Krawczyk, Archives of Metallurgy and Materials **60** (3), 1633-1638 (2015), DOI: 10.1515/amm-2015-0285 (online).

[2] K. Adamus, P. Lacki, Archives of Metallurgy and Materials **62** (4), 2399-2404 (2017), DOI: 10.1515/amm-2017-0353 (online).

[3] R. Konar, M. Mician, Archives of Foundry Engineering **17** (2), 35-38 (2017).

[4] Ch. Lin et al., Advances in Mechanical Engineering **8** (4), (2016), DOI: 10.1177/1687814016644127.

[5] R. Konar, M. Bohacik, M. Mician, Manufacturing Technology **16** (5), 955-961 (2016)

[6] J. Winczek, Procedia Engineering **136**, 108-113 (2016).

[7] J. Winczek, T. Skrzypczak, Archives of Metallurgy and Materials **61** (3), 1623-1634 (2016), DOI: 10.1515/amm-2016-0264.

[8] D. Bolibruchova, J. Macko, M. Bruna, Archives of Metallurgy and Materials **59** (2), 717-721 (2014)

[9] D.N. Collins, W. Alcheikh, Journal of Materials Processing Technology **55**, 85-90 (1995)

[10] M. Bruna, D. Bolibruchova, R. Pastircak, Archives of Foundry Engineering **17** (3), 23-26 (2017)

[11] M.J. Crook, G.R. Jordan, NDT international **23** (4), 221-227 (1990)

[12] A. Orlowicz, M. Mróz, A. Trytek, Archives of Foundry Engineering **7** (1), 13-18 (2007)